DOI: 10.1002/zaac.200700275

Trovacene Chemistry. 16 [1]
1,1a-Di([5]trovacenyl)-1,1,1a,1a-tetraphenyl-disiloxane: Electro- and Magneto-Communication Across a Si-O-Si Spacer

Christoph Elschenbroich[a,]*, Feng Lu[a], Olaf Burghaus[a], Klaus Harms[a], and Mathias Nowotny[b]

[a] Marburg, Fachbereich Chemie der Philipps-Universität
[b] Darmstadt, Institut für Anorganische Chemie der Technischen Hochschule

Received May 24th, 2007.

Dedicated to Professor Dieter Fenske on the Occasion of his 65th Birthday

Abstract. By means of lithiation and subsequent derivatization [5]trovacenyl-diphenylsilanol (**2**$^{\cdot}$), di([5]trovacenyl)tetraphenyl-disiloxane (**3**$^{\cdot\cdot}$), di([5]trovacenyl)tetramethyl-disiloxane (**4**$^{\cdot\cdot}$) and di([5]-trovacenyldimethylsilyl)methane (**6**$^{\cdot\cdot}$) have been prepared and characterized by X-ray diffraction (**2**$^{\cdot}$, **3**$^{\cdot\cdot}$, **6**$^{\cdot\cdot}$). Although the bond angles of the disiloxane bridges differ considerably, magnetic exchange interaction in these organometallic diradicals is practically unaffected as shown by fluid solution EPR spectroscopy. By way of contrast, electrocommunication clearly responds to change in the structure of the SiOSi spacer in that the redox splittings derived from cyclic voltammetry display the gradation $\delta E_{1/2}$ (0/−/2−) **4**$^{\cdot\cdot}$ < **6**$^{\cdot\cdot}$ < **3**$^{\cdot\cdot}$. It is proposed that in this order electronic polarizability in the intervening spacer increases thereby facilitating the transmission of electrostatic effects.

Keywords: Trovacene; Silanol; Disiloxane; Spin exchange coupling; Cyclic voltammetry

1 Introduction

Inorganic and organometallic polymers have received attention with regard to the possibility that they exhibit interesting materials properties such as rigidity, electrical conductivity, non-linear optical phenomena, or molecular ferromagnetism [2]. Whereas backbones composed of main group nonmetals (polysilanes, polysiloxanes, polyphosphazenes, polyborazylenes) have a long tradition metal-containing polymers, are of more recent vintage [2e, k]. The latter comprise two classes, namely polymers that incorporate organometallic units in their backbone, and those in which these units form substituents at the polymer chain. In the following we disclose the synthesis, structural elucidation, EPR spectra, magnetic susceptometry and cyclic voltammetry of a disiloxane which bears two paramagnetic [5]trovacenyl groups [3]. This molecule may be regarded as the smallest representative in the class of poly([5]trovacenyl)siloxanes and should lend itself to a study of the extent of intramolecular intermetallic communication mediated by a Si-O-Si bridge. Polysiloxanes decorated with paramagnetic sandwich units could lead to super paramagnetic nanostructures [2b]; they also could serve in studies of motional properties since the latter modulate the ^{51}V hyperfine tensor with attendant effects on the linewidths as a function of m_I (^{51}V). The work described here is part of our systematic investigation of electron spin-spin coupling and redox splitting in oligotrovacenyls as a function of the nature of the spacers [4].

2 Results and Discussion

The most common access to disiloxanes proceeds via the sequence $R_3SiCl \xrightarrow{H_2O} R_3SiOH \xrightarrow[-H_2O]{2\times} R_3SiOSiR_3$. Herein, the ease of dehydration is controlled by the nature of R. Typically, the condensation of triphenylsilanol calls for concentrated acid or for strongly alkaline media and elevated temperature [5, 6], conditions which are detrimental to the trovacene unit. We nevertheless prepared [5]trovacenyldiphenylsilanol (**2**$^{\cdot}$) (Scheme 1), a potential precursor to di([5]trovacenyl)tetraphenyl- disiloxane, because silanols present remarkable structural features imposed by strong hydrogen bonding [6]. The molecular structure of the silanol **2**$^{\cdot}$ crystallized from ethanol is presented in Figure 1, bond lengths and bond angles are collected in Table 1. Contrary to triphenylsilanol, which in the crystal forms hydrogen bonded tetramers [5], [5]trovacenyldiphenylsilanol generates hydrogen bonded dimers, which incorporate an additional molecule of ethanol.

The larger size of the trovacenyl compared to the phenyl substitutent at silicon is an obvious explanation for the lower degree of aggregation in **2**$^{\cdot}$ compared to triphenylsilanol. Considering the O-H···O distances (2.74, 2.74 Å) and angles (167°, 170°), the hydrogen bonds in **2**$^{\cdot}$ are moderately

---

* Prof. Dr. C. Elschenbroich
Fachbereich Chemie der Universität
D-35032 Marburg
E-mail: eb@chemie.uni-marburg.de

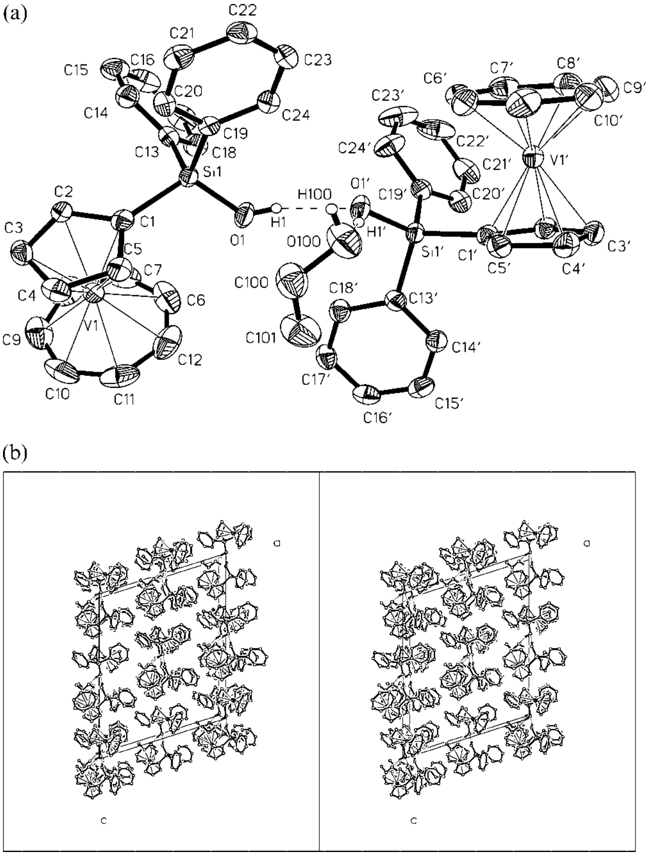

Figure 1 (a) Molecular structure of [5]trovacenyl-diphenylsilanol ($\mathbf{2}^{\cdot}$) in a crystal grown from ethanol (50 % probability ellipsoids). Two units of $\mathbf{2}^{\cdot}$connected by a $\mathrm{HSiO\text{-}H\cdots\underset{H}{O}Si}$ hydrogen bond and interacting with a C_2H_5OH molecule are shown. (b) Stereoview of the unit cell illustration the packing of the dimers $(\mathbf{2}^{\cdot})_2\cdot C_2H_5OH$.

Table 1 Selected bond lengths /Å and angles /° for [5]trovacenyl-diphenylsilanol $\mathbf{2}^{\cdot}$ as found for $(\mathbf{2}^{\cdot})_2\cdot C_2H_5OH$.

Si1−C1	1.861(3)	V1−C6	2.171(4)
Si1−C13	1.869(4)	V1−C7	2.172(4)
Si1−C19	1.877(3)	V1−C8	2.180(5)
Si1−C (mean)	1.869(3)	V1−C9	2.188(5)
V1−C1	2.275(3)	V1−C10	2.185(5)
V1−C2	2.260(3)	V1−C11	2.178(4)
V1−C3	2.268(3)	V1−C12	2.172(4)
V1−C4	2.255(4)	V1−C_7 ring (mean)	2.178(4)
V1−C5	2.247(4)	V1−C_7 (centroid)	1.468(1)
V1−C_5 ring (mean)	2.261(3)	C6−C7	1.382(7)
V1−C_5 (centroid)	1.913(2)	C6−C12	1.414(8)
Si1−O1	1.626(2)	C7−C8	1.410(7)
O1−H1	0.78(5)	C8−C9	1.394(7)
C1−C2	1.433(5)	C9−C10	1.372(8)
C1−C5	1.426(5)	C10−C11	1.394(8)
C2−C3	1.401(5)	C11−C12	1.406(7)
C3−C4	1.406(6)	C−C (mean for C_7)	1.396(8)
C4−C5	1.422(5)	O1−H1 ···O1′	2.742(3)
C−C (mean for C_5)	1.417(5)	O1′−H1′ ··· O100	2.740(4)

O1-Si1-C1	109.85(15)	O1-Si1-C1-C5	45.8(3)
O1-Si1-C13	109.21(15)	C13-Si1-C1-C5	165.6(3)
C1-Si1-C13	109.31(15)	C19-Si1-C1-C5	−76.5(3)
O1-Si1-C19	110.50(14)	O1-Si1-C1-C2	−137.5(3)
C1-Si1-C19	110.63(15)	Si1-C1-C2-C3	−177.4(3)
C13-Si1-C19	107.29(15)	C5-C1-C2-C3	0.0(4)
Si1-O1-H1	120(3)	O1-Si1-C13-C14	−172.7(3)
C5-C1-Si1	128.6(3)	C1-Si1-C13-C14	67.1(3)
C2-C1-Si1	126.3(3)	C19-Si1-C13-C14	−52.9(3)
C14-C13-Si1	121.5(3)	Si1-C13-C14-C15	179.7(3)
C5-C1-C2	105.0(3)	C13-C14-C15-C16	−1.5(6)
C14-C13-C18	116.6(3)	O1-Si1-C19-C20	−149.3(3)
C20-C19-C24	116.8(3)	C1-Si1-C19-C20	−27.4(3)
C20-C19-Si1	122.3(3)	Torsion C_7 ring (mean)	0.0(0)
O1−H1 ··· O1′	167	Torsion C_5 Rring (mean)	0.0(0)
O1′−H1′ ··· O100	170		

strong [7]. Interestingly, despite differences in environment the hydrogen bonds O(1)-H(1)···O(1′) and O(1′)-H(1′)···O(100) are of almost equal strength. A totally different packing of $\mathbf{2}^{\cdot}$ is encountered if crystals are grown from benzene/petroleum ether (Figure 2, Table 2). No solvent molecules are incorporated and significant intermolecular hydrogen bonding is absent in this case.

At best very weak interactions O-H···C_π, C-H···C_π can be spotted between silanol- and cycloheptatrienyl hydrogen atoms and the π-perimeter of a neighboring η^7-C_7H_7 ligand; they are marked in Figure 2. Thus, as taken from Table 2, the distances *d*(H···C) are only slightly smaller than the sum of van der Waals radii for C and H (≈ 2.90 Å [7]). The fact that the more acidic silanol OH function gives rise to a smaller *d*(H···C) value than the η^7-C_7H_7 donor, may be regarded as evidence for the existence of hydrogen bonding to C_π acceptors [8].

The absence of O-H···O hydrogen bonding for crystalline $\mathbf{2}^{\cdot}$ contrasts with triphenylsilanol which forms a hydrogen bonded cyclic tetramer $(Ph_3SiOH)_4$ and additionally incorporates one molecule of ethanol yielding a pentagon of hydrogen bonded oxygen atoms $(Ph_3SiOH)_4\cdot EtOH$ [5]. As a transition metal derivative of triphenylsilanol compound $\mathbf{2}^{\cdot}$ resembles $Ph_2[\eta^6\text{-}PhCr(CO)_3]Si(OH)$; for the latter the siloxy hydrogen atom could not be precisely located and intermolecular hydrogen $\mathrm{HSiO\text{-}H\cdots\underset{H}{O}Si}$ bonding was not address [9].

Since dehydration of $\mathbf{2}^{\cdot}$ failed, we prepared the target compound $\mathbf{3}^{\cdot\cdot}$ by the path given in Scheme 1. The side product [5]trovacenyldiphenylsiloxy-diphenylsilanol $\mathbf{5}^{\cdot}$ probably stems from single C-Si coupling and hydrolysis of the remaining Si-Cl bond during workup. X-ray crystallography performed on crystals of $\mathbf{5}^{\cdot}$ yielded the structure which is depicted in Figure 3; it merely served unequivocal product identification and will not be discussed in detail here.

The structure of the title compound 1,1a-di([5]trovacenyl)-1,1,1a,1a-tetraphenyldisiloxnae ($\mathbf{3}^{\cdot\cdot}$) is shown in Figure 4, bond lengths and angles are listed in Table 3. Obviously the structure of $\mathbf{3}^{\cdot\cdot}$ should be compared to that of hexaphenyldisiloxane (**7**). The latter has been reported to be centrosymmetric, the SiOSi fragment being strictly linear and featuring the bond length Si-O = 1.616 (1) Å [10]. The SiOSi backbone in $\mathbf{3}^{\cdot\cdot}$ differs in that it is slightly bent [168.4(2)°], correspondingly, the Si-O bonds are a little longer [1.6212(7) Å] than those in **7**. If the SiOSi segment in $\mathbf{3}^{\cdot\cdot}$ is approximated to be linear, the structure may be

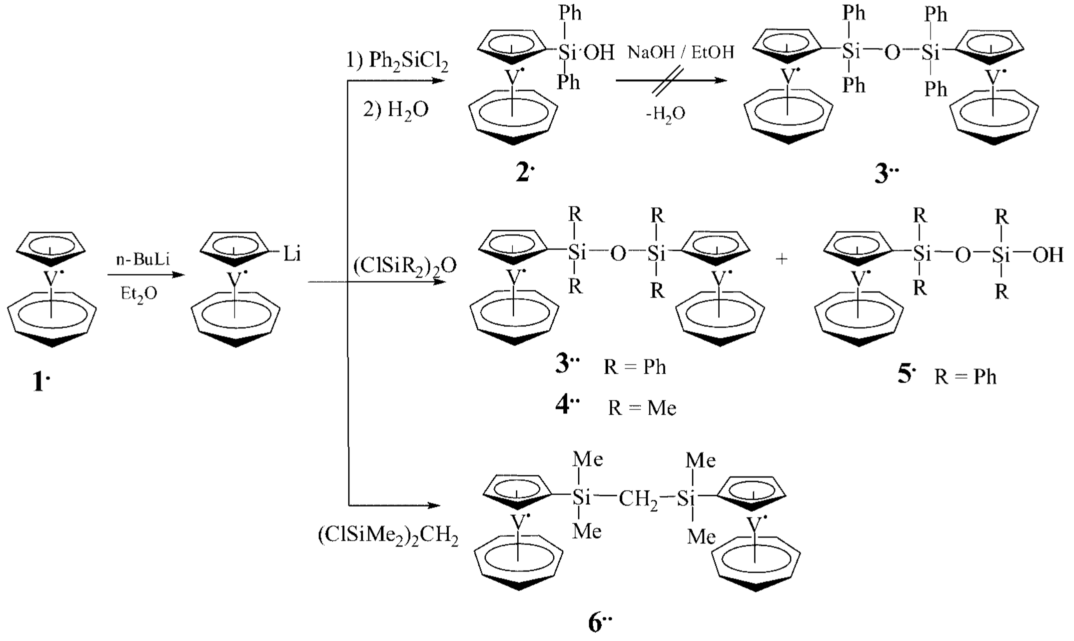

Scheme 1

designated *syn* clinal. With regard to the Si-C_{ipso} bonds, the [5]trovacenyl groups assume conformations which maximize the V1···V1a distance [7.85 Å] thereby minimizing inter-trovacene repulsion. Intermolecular forces must also be reckoned with, however, as has been demonstrated for the closely related 1,1a-diferrocenyl-1,1,1a,1a-tetramethyldisiloxane (**8**) which exhibits a nearly eclipsed conformation when viewed along the SiOSi axis [angle 159.9(2)°] whereas a staggered form is adopted in a cocrystal **8**·ferrocene [SiOSi 141.5(1)°] [11]. This study once again illustrates the flexibility of the disiloxane linkage and suggests, that the structure of **3**·· in solution may differ considerably from that in the solid state.

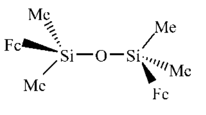

8

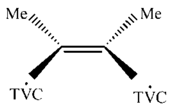

9··

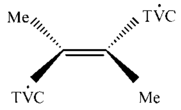

10··

The methyl analog of **3**··, namely 1,1a-di([5]trovacenyl)-1,1,1a,1a-tetramethyldisiloxane (**4**··) is expected to display structural differences of the Si-O-Si segment which could have an impact on intramolecular communication; **4**·· was therefore also synthesized and subjected to an X-ray diffraction study (Figure 5, Table 4). The most important feature of **4**·· is the more strongly bent disiloxane bridge (θ SiOSi = 146.6°).

Intramolecular **magnetocommunication** in **3**·· manifests itself most clearly in the **EPR** hyperfine pattern observed in fluid solution (Figure 6); 15 components separated by a(^{51}V, **3**··)/2, which strongly deviate in intensity from the 1:2:3···8:7···1 distribution attest to the region of intermediate exchange on the a(^{51}V) time scale [14]. Spectral simulation furnished the value $|J_{EPR}(\mathbf{3}^{\cdot\cdot})| = 0.070\ \mathrm{cm}^{-1}$ for the exchange parameter. This corresponds to $|J| = 75$ mT and implies, that $|J_{EPR}(\mathbf{3}^{\cdot\cdot})| \approx 10$ a(^{51}V, **1**·). If one strives at putting the exchange coupling constant $J_{EPR}(\mathbf{3}^{\cdot\cdot})$ in perspective, comparing it with values obtained for hydrocarbon spacers, *Z*-2,3-di([5]trovacenyl)-2-butene (**9**··) is the species of choice in that $|J_{EPR}(\mathbf{9}^{\cdot\cdot})| = 0.052\ \mathrm{cm}^{-1}$ [14].

Accordingly the three-atom disiloxane spacer matches the two atom *Z*-alkene unit in the ability to mediate electron-spin exchange-coupling. As a caveat it must be stated that it is not only the chemical nature of the spacer but also steric particularities which govern the extent of exchange coupling. This is illustrated by the fact that for the isomer *E*-2,3-di([5]trovacenyl)-2-butene (**10**··) exchange coupling is much more extensive $|J(\mathbf{10}^{\cdot\cdot})| \approx 20\ |J(\mathbf{9}^{\cdot\cdot})|$. This has been attributed to the greater ease of **10**·· compared to **9**·· to achieve coplanarity of the cyclopentadienyl- and alkene π-electron systems. The dramatic difference in exchange-coupling efficiency for the isomers **9**·· and **10**·· strongly suggests that π-delocalization plays an important role, as the inter-vanadium distances are very similar and the number of intervening bridge atoms are identical for **9**·· and **10**··.

The extensive SiOSi bond angle widening to approach linearity and the short SiO bonds in **3**·· suggest the presence of two neighboring Si=O double bonds. Therefore compound **3**·· bears strong resemblance to the [2]cumulene 1,3-diferrocenylallene (R)FcC=C=CFc(R) in that the spacer features two orthogonal π- bonds [15]. As far as π-bonding is concerned, odd cumulenes with C_3, C_5, C_7 backbones are nonconjugated and electronically decoupled. It therefore does not come as a surprise that exchange coupling in **3**·· ($|J_{EPR}| = 0.070\ \mathrm{cm}^{-1}$) is much weaker than that in 1,4-di[5]-trovacenylbutadiyne (**11**··) ($|J_{EPR}| = 0.56\ \mathrm{cm}^{-1}$) [16] despite

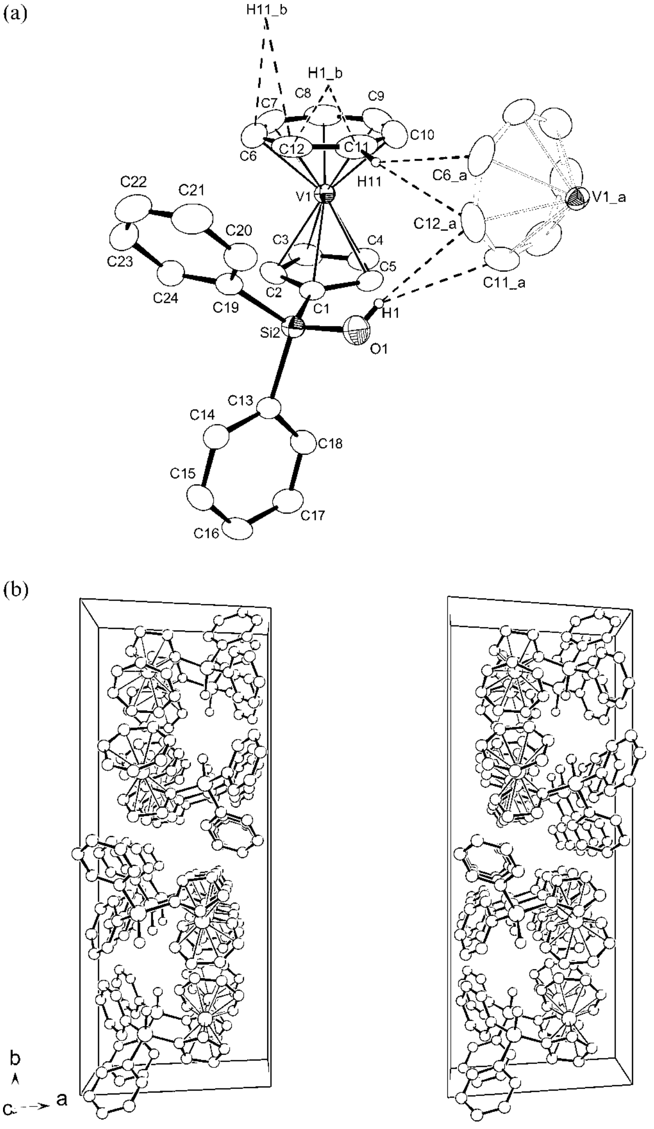

Figure 2 (a) Molecular structure of [5]trovacenyldiphenylsilanol ($\mathbf{2}^{\cdot}$) in a crystal grown from petroleum ether/benzene (50 % probability ellipsoids). Weak intermolecular hydrogen bonds are indicated by dotted lines. (b) Stereoview of the unit cell.

Table 2 Selected bond lengths /Å and angles /° for [5]trovacenyldiphenylsilanol ($\mathbf{2}^{\cdot}$) as found for crystals devoid of included solvent molecules.

C1−Si2	1.856(2)	C6−V1	2.169(2)
C13−Si2	1.874(2)	C7−V1	2.171(2)
C19−Si2	1.865(2)	C8−V1	2.179(2)
Si1−C(mean)	1.865(2)	C9−V1	2.178(2)
C1−V1	2.270(2)	C10−V1	2.177(2)
C2−V1	2.248(2)	C11−V1	2.174(2)
C3−V1	2.249(2)	C12−V1	2.177(2)
C4−V1	2.246(2)	V1−C_7 ring (mean)	2.175(2)
C5−V1	2.247(2)	C6−C12	1.395(3)
C_5−V1 ring (mean)	2.252(2)	C6−C7	1.388(3)
O1−Si2	1.6360(13)	C7−C8	1.373(3)
O1−H1	0.74(3)	C8−C9	1.389(3)
C1−C2	1.426(2)	C9−C10	1.403(4)
C1−C5	1.430(3)	C10−C11	1.409(4)
C2−C3	1.403(3)	C11−C12	1.412(4)
C3−C4	1.404(3)	C−C (mean for C_7)	0.0(0)
C4−C5	1.413(3)	C−C (mean for C_5)	0.0(0)
d(H···C)	2.75(3)		

O1-Si2-C1	109.32(8)	C20-C19-Si2	119.28(14)
O1-Si2-C13	106.80(7)	C5-C1-Si2-O1	14.58(14)
C1-Si2-C13	109.05(7)	C5-C1-Si2-C13	−101.84(14)
O1-Si2-C19	108.99(8)	C5-C1-Si2-C19	135.90(14)
C1-Si2-C19	112.63(7)	C2-C1-Si2-O1	−170.99(14)
C19-Si2-C13	109.88(7)	C14-C13-Si2-C1	−135.57(13)
Si2-O1-H1	118(3)	C5-C1-C2-C3	0.1(2)
C5-C1-Si2	126.00(13)	C14-C13-Si2-O1	106.41(14)
C2-C1-Si2	128.28(13)	C24-C19-Si2-C13	−64.4(2)
C14-C13-Si1	123.02(12)	Si2-C13-C14-C15	−179.30(13)
C3-C1-C2	109.5(2)	C13-C14-C15-C16	1.1(3)
C14-C13-C18	117.1(2)	C20-C19-Si2-O1	2.9(2)
C20-C19-C24	117.5(2)	C20-C19-Si2-C1	−118.60(14)
Si2-C1-C5-C4	175.35(12)	Torsion C_7 ring (mean)	0.0(0)
		Torsion C_5 ring (mean)	0.0(0)

of the fact that in $\mathbf{11}^{\cdot\cdot}$ a C_4 spacer is encountered whereas $\mathbf{3}^{\cdot\cdot}$ contains a C_3 spacer. Conjugation of two neighboring triple bonds is of course uninhibited and rotationally invariant. Supposedly the as yet unknown [3]cumulene spacered dinuclear complex $(C_7H_7)V(C_5H_4\text{-}CH{=}C{=}C{=}CH\text{-}H_4C_5)V(C_7H_7)$ will surpass $\mathbf{3}^{\cdot\cdot}$ in its propensity to mediate exchange interaction because it features 1,3-butadiene conjugation.

Disiloxanes are known to differ in their Si-O-Si angles θ dependent on the substituents at the Si atoms. Whereas for $Ph_3SiOSiPh_3$ $\theta = 180°$ applies [10], in siloxanes bearing less bulky methyl groups the bridge deviates from linearity (example: $FcMe_2SiOSiMe_2Fc$, θ (SiOSi) = 159.9° [11]). In order to explore whether lifting the orthogonality of the two SiO double bond contributions in a nonlinear disiloxane would lead to a rise in exchange coupling, we prepared compound $\mathbf{4}^{\cdot\cdot}$ (Scheme 1) which features the angle θ (SiOSi) = 146.6° (Figure 5, Table 4). Surprisingly the fluid solution EPR spectrum of $\mathbf{4}^{\cdot\cdot}$ (Figure 6) is superimposable on that of $\mathbf{3}^{\cdot\cdot}$ ($|J(\mathbf{4}^{\cdot\cdot})| = 0.076\ \text{cm}^{-1} \approx 81$ mT, i.e. the pronounced difference in SiOSi angles does not lead to a magnetostructural effect. If one would be pressed to come up with an explanation one could argue that upon decreasing the SiOSi angles two contributions cancel: (1) proceeding from the 3 atom hetero-cumulene electronic structure (180°) to a participation of an allyl structure (146.6°) increases π conjugation and exchange coupling mediated by a π path; (2) the decrease in SiOSi angle will decrease the s character of the σ bonds thereby weakening magnetic communication transmitted by a σ path. A different type of reasoning is based on the fact that the SiOSi angle bending potential in the range $130° < \theta < 230°$ is very flat (inversion barrier 1.34 kJ mol^{-1} [17]). This will serve to eliminate the structural differences observed for the solid state in that thermally activated inversion of the SiOSi bridge can occur, irrespective of the substitutent at the Si atoms. Steric effects will therefore not become manifest. Finally, the notion of replacing the lone pairs at the central oxygen atom of the disiloxane bridge by σ-bonding pairs led us to the synthesis of di[[5]trovacenyldimethylsilyl]methane ($\mathbf{6}^{\cdot\cdot}$) (Scheme 1)

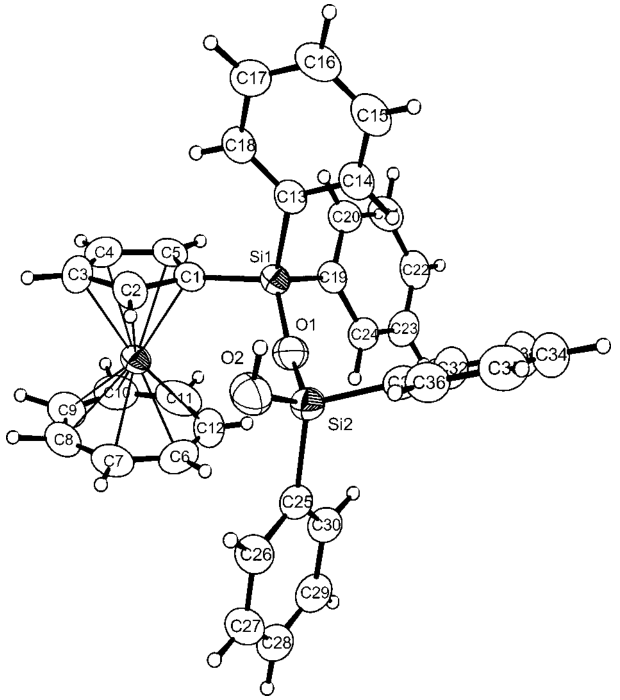

Figure 3 Molecular structure of [5]trovacenyldiphenylsiloxy-diphenylsilanol (**5**$^{\cdot}$) in the crystal (50 % probability ellipsoids). Parameters for the disiloxane bridge: Si1−O1 1.635(2) Å; Si2−O1 1.622(2) Å; Si2−O2 1.618(2) Å; Si1-O1-Si2 155.03(11)°.

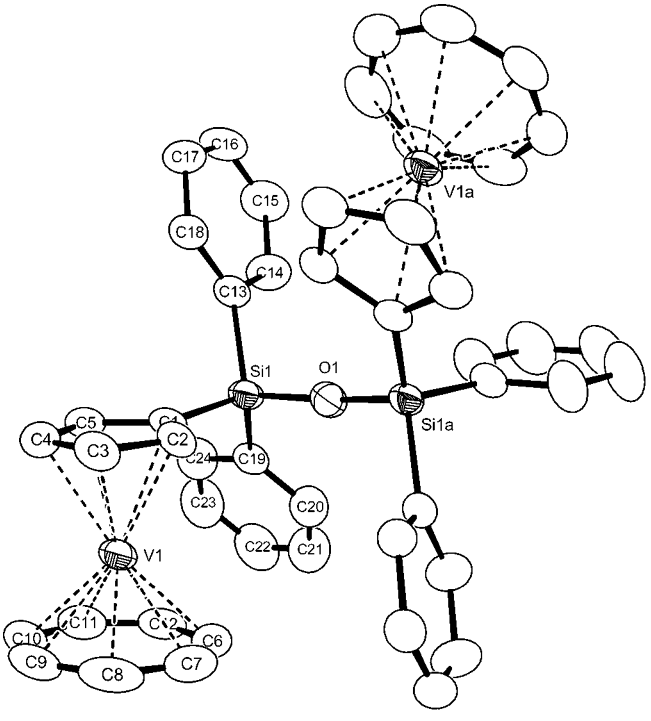

Figure 4 Molecular structure of 1,1a-Di([5]trovacenyl)-1,1,1a,1a−tetraphenyl-disiloxane (**3**$^{\cdot\cdot}$) in a crystal grown from petroleum ether/benzene (50 % probability ellipsoids).

Table 3 Selected bond lengths /Å and angles /° for 1,1a-Di([5]trovacenyl)-1,1,1a,1a-tetraphenyl-disiloxane (**3**$^{\cdot\cdot}$).

C1−Si1	1.855(3)	C1−C2	1.423(4)
O1−Si1a	1.6210(7)	C1−C5	1.433(4)
O1−Si1	1.6210(7)	C2−C3	1.399(4)
C13−Si1	1.872(2)	C3−C4	1.411(4)
C19−Si1	1.861(3)	C4−C5	1.403(4)
V1−C1	2.281(2)	C−C (mean for C_5)	1.413(4)
V1−C2	2.256(2)	C6−C7	1.413(6)
V1−C3	2.257(3)	C6−C12	1.402(5)
V1−C4	2.252(3)	C7−C8	1.385(6)
V1−C5	2.259(2)	C8−C9	1.409(5)
V1−C_5 ring (mean)	2.256(3)	C9−C10	1.389(5)
V1−C6	2.185(3)	C10−C11	1.396(5)
V1−C7	2.175(3)	C11−C12	1.398(4)
V1−C8	2.182(3)	V1−C11	2.183(3)
V1−C9	2.178(3)	V1−C12	2.183(4)
V1−C10	2.177(3)	V1−C_7 ring (mean)	2.180(4)
V1 ··· V2	7.8532(7)		

C2-C1-Si1	125.6(2)	C2-C1-C5	105.5(2)
C5-C1-Si1	128.5(2)	Si1a-O1-Si1	168.5(2)
O1-Si1-C19	107.37(12)	C1-Si1-C19	114.88(11)
O1-Si1-C1	108.11(11)	O1-Si1-C13	108.48(8)
C1-Si1-C13	109.99(11)	C19-Si1-C13	107.83(12)
C5-C1-Si1-C19	177.1(2)	C2-C1-Si1-C13	−113.3(2)
Si1a-O1-Si1-C19	−154.90(9)	Si1-C19-C24-C23	−178.9(3)
Si1a-O1-Si1-C13	88.82(10)	Si1a-O1-Si1-C1	−30.41(8)

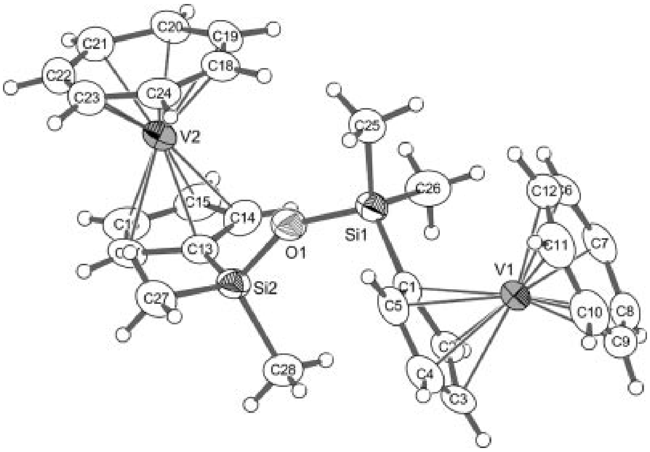

Figure 5 Molecular structure of di[5]trovacenyltetramethyl-disiloxane (**4**$^{\cdot\cdot}$) in a crystal grown from petroleum ether / benzene (50 % probability ellipsoids).

and its EPR study (Figure 6). Although no X-ray diffraction study was carried out for **6**$^{\cdot\cdot}$, it can be assumed with certainty that the bridging angle Si-C-Si will be close to tetrahedral (109.5°). The EPR spectrum of **6**$^{\cdot\cdot}$in fluid solution and its simulation supplied the exchange parameter $|J(\mathbf{6}^{\cdot\cdot})| = 0.076\ \mathrm{cm}^{-1}$ (81 mT) which differs insignificantly from those found for **3**$^{\cdot\cdot}$ and **4**$^{\cdot\cdot}$. Apparently, the siloxane Si-O-Si and carbosilane Si-CH_2-Si spacers are equally effective in promoting exchange coupling in that O (lone pair)-Si conjugation in **3**$^{\cdot\cdot}$ and **4**$^{\cdot\cdot}$ is replaced by CH-Si hyperconjugation in **6**$^{\cdot\cdot}$.

Table 4 Selected bond lengths /Å and angles /° di[5]trovacenyl-tetramethyl-disiloxane $\mathbf{4}^{\cdot\cdot}$.

C1−C2	1.424(4)	C1−Si1	1.855(3)
C1−C5	1.424(4)	O1−Si1	1.637(2)
C2−C3	1.401(4)	O1−Si2	1.631(2)
C3−C4	1.389(5)	C13−Si2	1.857(3)
C4−C5	1.411(4)	V1−C(1)	2.256(3)
C−C (mean for C_5)	1.409(4)	V1−C2	2.241(3)
C6−C7	1.394(5)	V1−C3	2.256(2)
C6−C12	1.395(5)	V1−C4	2.267(3)
C7−C8	1.407(5)	V1−C5	2.256(3)
C8−C9	1.387(6)	V1−C5 ring (mean)	2.255(3)
C9−C10	1.399(6)	O1-Si1-C1	108.33(10)
C10−C11	1.396(6)	C5-C1-Si1	126.5(2)
C11−C12	1.388(5)	Si2-O1-Si1	146.61(13)
V1−C6	2.177(2)	Si2-O1-Si1-C26	76.1(3)
V1−C7	2.178(3)	C2-C1-C5	105.6(2)
V1−C8	2.170(3)	C2-C1-Si1	127.7(2)
V1−C9	2.167(3)	O1-Si1-C26	108.44(14)
V1−C10	2.175(3)	O1-Si1-C25	107.11(12)
V1−C11	2.182(3)	C26-Si1-C1	110.32(14)
V1−C12	2.180(3)	Si2-O1-Si1-C25	−164.1(2)
V1-C_7 ring (mean)	2.177(3)	Si2-O1-Si1-C1	−43.6(3)
V1···V2	8.8206(9)	C5-C1-Si1-O1	−81.1(2)
C2-C1-Si1-O1	92.1(2)		

Exchange coupling in oligotrovacenyls can be studied by two methods which are complementary with regard to the strength of this magnetic interaction. Owing to the magnitude of hyperfine splitting in parent trovacene [$|a(^{51}V, \mathbf{1}^{\cdot})| = 6.98$ mT $= 0.0065$ cm^{-1}] EPR analysis can be applied for $0.001 \lesssim |J| \lesssim 1$ cm^{-1} whereas magnetic susceptometry requires $|J| \gtrsim 1$ cm^{-1}. Therefore, the very small exchange coupling constants determined for $\mathbf{3}^{\cdot\cdot}$, $\mathbf{4}^{\cdot\cdot}$, and $\mathbf{6}^{\cdot\cdot}$ by fluid solution EPR preclude an application of magnetic susceptometry. It should be mentioned that in cases of exceedingly weak intramolecular exchange coupling reliably quantified by EPR, the interpretation of χ-T traces is complicated by the problem of disentangling intra- and intermolecular contributions. Quite frequently, in the solid state intermolecular V···V distances are shorter than the intramolecular ones and the χ-T curve then reflects a magnetic exchange interaction whose origin is not strictly intramolecular. This problem has been dealt with previously in the case of 1,4-di([5]trovacenyl)butadiyne $(C_7H_7)V(C_5H_4(\text{-C}\equiv\text{C-C}\equiv\text{C-}(C_5H_4)V(C_7H_7)$ [16]. It may even be argued that in the solid state, the differentiation intra/intermolecular becomes blurred and we therefore refrain from presenting here the χ-T curves for $\mathbf{3}^{\cdot\cdot}$, $\mathbf{4}^{\cdot\cdot}$, and $\mathbf{6}^{\cdot\cdot}$ and their multiparameter fits.

Electrocommunication in oligonuclear complexes may be gauged from redox splittings, i.e, the differences in the potentials of successive electron transfer steps. The cyclic voltammograms (CV) for $\mathbf{3}^{\cdot\cdot}$, $\mathbf{4}^{\cdot\cdot}$ and $\mathbf{6}^{\cdot\cdot}$ are presented in Figure 7, relevant data are collected in Table 5. CV traces for oligonuclear trovacenes usually show three clearly separated regions: vanadium centered reduction ($-3.0 \lesssim E \lesssim -2.4$ V), vanadium-centered oxidation ($0 \lesssim E \lesssim 0.5$ V) and irreversible further oxidation ($E \gtrsim 1.0$ V). From the electrocommunication point of view redox splitting $\delta E_{1/2}$ rather than absolute peak positions are of prime concern. In the series under investigation redox splitting is partially resolved only in the cathodic region for which the gradation $\delta E_{1/2}$ (0/−/2−) $\mathbf{3}^{\cdot\cdot} > \mathbf{6}^{\cdot\cdot} > \mathbf{4}^{\cdot\cdot}$ is observed. In search for an electrostructural correlation one notices that $\mathbf{3}^{\cdot\cdot}$ contains a nearly linear disiloxane bridge with the shortest Si-O bond lengths in the series and a partial conversion of the oxygen lone pairs into O-Si π−bonding electron pairs. Possibly it is the attendant increase in polarizability of these electrons which fosters the transmission of an electrostatic effect ac-

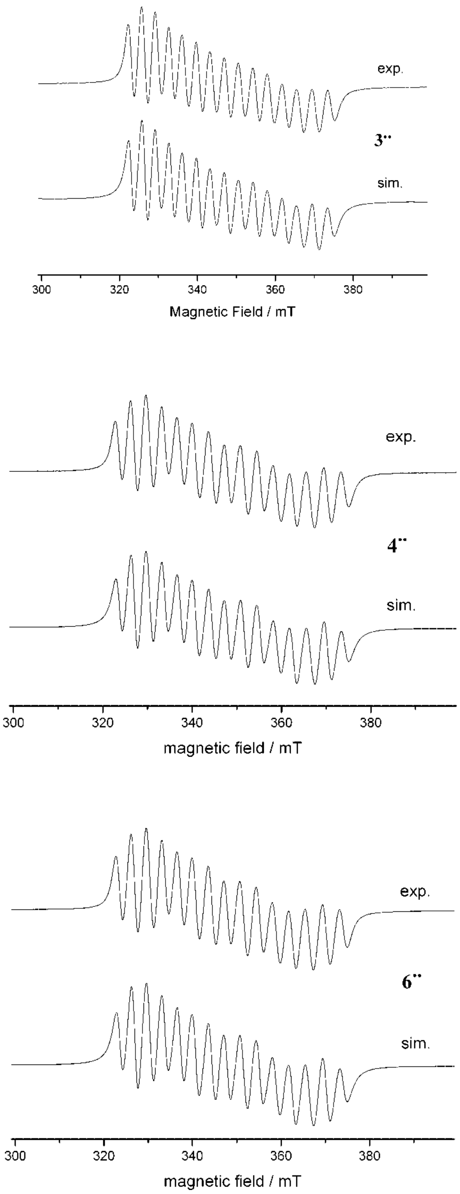

Figure 6 Experimental and simulated EPR spectra for the biradicals $\mathbf{3}^{\cdot\cdot}$, $\mathbf{4}^{\cdot\cdot}$, and $\mathbf{6}^{\cdot\cdot}$ (X-band, toluene, 290 K). $\mathbf{3}^{\cdot\cdot}$: $g_{iso} = 1.986$, $a(^{51}V) = 7.28$ mT, $|J_{EPR}| = 75$ mT (0.070 cm^{-1}), line width = 3.3 mT, $\alpha = -0.77$, $\beta = -0.004$, $\gamma = 2.8$, $\chi^2 = 0.06$, α, β, γ are the coefficients in the line width equation which, in spectral simulations allow for m_I dependence of the line shape [12]. $\mathbf{4}^{\cdot\cdot}$: $g_{iso} = 1.986$, $a(^{51}V) = 7.20$ mT, $|J_{EPR}| = 81$ mT (0.076 cm^{-1}), line width = 3.2 mT, $\alpha = -0.51$, $\beta = -0.037$, $\gamma = 0.89$, $\chi^2 = 0.083$. $\mathbf{6}^{\cdot\cdot}$: $g_{iso} = 1.986$, $a(^{51}V) = 7.20$ mT, $|J_{EPR}| = 83$ mT (0.077 cm^{-1}), line width = 3.1 mT, $\alpha = -0.52$, $\beta = -0.034$, $\gamma = 0.92$, $\chi^2 = 0.084$.

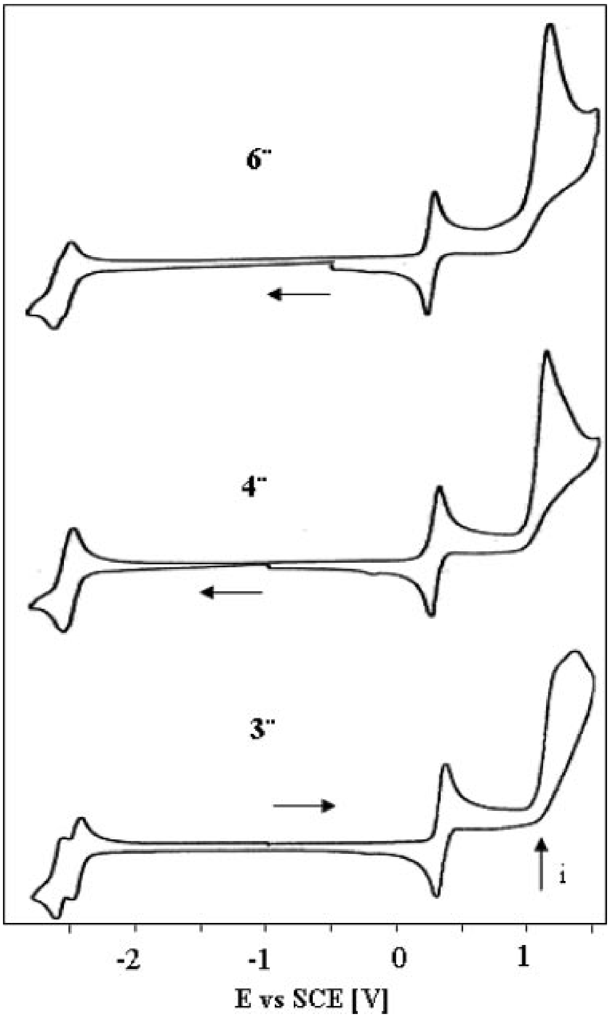

Figure 7 Cyclic voltammetry traces for the complexes **3**$^{\cdot\cdot}$, **4**$^{\cdot\cdot}$, and **6**$^{\cdot\cdot}$ (DME, $(n\text{-Bu})_4N(ClO_4)$, −40 °C, v = 100 mV s^{-1}, SCE).

Table 5 Electrochemical data from cyclic voltammetry for the complexes **3**$^{\cdot\cdot}$, **4**$^{\cdot\cdot}$, and **6**$^{\cdot\cdot}$.

Spacer	$-SiMe_2CH_2SiMe_2$- **3**$^{\cdot\cdot}$	$-SiMe_2OSiMe_2$- **4**$^{\cdot\cdot}$	$-SiPh_2OSiPh_2$- **6**$^{\cdot\cdot}$
$E_{1/2}$ (-/2-) / V	−2.56	−2.53	−2.54
ΔE_p / mV	50	50	58
$E_{1/2}$ (0/-) / V	−2.48	−2.49	−2.41
ΔE_p / mV	50	50	56
$E_{1/2}$ (+/0) / V	0.25	0.24	0.28
ΔE_p /mV	54	54	58
Ep,a (n+/+) / V	1.08	1.07	1.18
Ep,c (ECE) / V	−0.18	−0.20	−0.20
$\delta E_{1/2}$ (0/-/2-) / mV	82	32 (estimated)	130

General conditions: working electrode: glassy carbon; E vs SCE; solvent: DME; 0.1 m TBAP; T = −40°.

ross this bridge, resulting in a detectable redox splitting. In a related fashion the smaller redox splitting observed for **6**$^{\cdot\cdot}$ could be traced to CH-Si hyperconjugation. The fact that redox splitting for reduction exceeds that for oxidation is plausible because V *d*-orbital expansion upon reduction brings the charges into closer proximity whereas *d*-orbital contraction during oxidation tends to separate the charges. Note that the redox processes at trovacene are highly metal centered as the HOMO of **1**$^{\cdot}$ is almost exclusively of Vd_{z2} character.

In **conclusion**, the work described here illustrates that modifying the nature of a spacer, keeping the number of spacer atoms constant not necessarily has a pronounced effect on the extent of the magnetic exchange interaction. Further studies on bi[5]trovacenyls separated by three-atom spacers will reveal, whether the near identity of the J values found for **3**$^{\cdot\cdot}$, **4**$^{\cdot\cdot}$, and **6**$^{\cdot\cdot}$ is accidental or whether the response of intramolecular electron-spin exchange coupling to changes of the spacer structure is smaller than surmised originally. Electrocommunication, on the other hand, is affected significantly as demonstrated by the redox splittings derived from cyclic voltammetry.

Experimental Section

All chemical manipulations and physical measurements were performed in an atmosphere of purified dinitrogen or argon in dry and degassed solvents employing standard Schlenk techniques [16]. Trovacene (η^7-C_7H_7)V(η^5-C_5H_5) (**1**$^{\cdot}$) [19] and $(ClSiMe_2)_2CH_2$ [20] and were prepared as described in the literature.

X-ray data collection

Single crystals were mounted at the top of a glass capillary in a drop of inert oil under a flow of cold gaseous nitrogen. The data were collected with a STOE IPDS2 diffractometer employing Mo Kα radiation (λ = 0.71073 Å). The structures were solved by direct methods. Full-matrix least-squares on F^2 were performed as structure refinements. All non-hydrogen atoms were refined anisotropically. Crystal data, technical programs, as well as software were listed in Table 6. The corresponding deposition numbers for **2**$^{\cdot}$, **3**$^{\cdot\cdot}$, **4**$^{\cdot\cdot}$, and **5**$^{\cdot}$ are CCDC 646027/646028, 646030, 646031, and 646029, respectively. Copies of data may be obtained free of charge on application to CCDC, 12 Union Road, Cambridge CB2 1EZ, UK (http://www.ccdc.cam.ac.uk).

[5]Trovacenyl-diphenylsilanol (2$^{\cdot}$)

To a solution of trovacene (**1**$^{\cdot}$) (860 mg, 4.15 mmol) in 150 ml Et_2O, n-butyl lithium (2.6 ml, 4.16 mmol, 1.6 M/hexane) was added and stirred at room temperature overnight to give a red-brown solution. After cooling to 0 °C, Ph_2SiCl_2 (0.22 ml, 1.0 mmol) was added dropwise in 1 h, then the mixture was warmed to r.t. and more Ph_2SiCl_2 (0.22 ml, 1.0 mmol) was added. The mixture was stirred overnight at room temperature, filtered through Celite and freed of all the volatiles. Purification by chromatography (Al_2O_3, 2×30 cm, eluted by EtOH/Et_2O) gave **2**$^{\cdot}$ as a purple solid. The single crystal suitable for X-ray diffraction was grown from saturated ethanol solution. EPR: X-band, toluene, 290 K, $A_{iso}(^{51}V)$ = 72.6 G, g_{iso} = 1.9834. Yield: 220 mg (0.54 mmol, 13 %).

Elemental analysis: $C_{24}H_{22}OSiV$ (405.26): calcd C 71.12, H 5.43; found C 69.13, H 5.78 %. EI-MS (70 eV) *m*/*z* = 405 [M^+] (48 %), 207 [TVC^+] (100 %).

Table 6 Crystallographic data of **2**·, **3**··, **4**··, and **5**·.

	2 **2**· EtOH	**2**· PE/benzene	**3**·· · 1/2 C_6H_6	**4**··	**5**·
crystal size /mm	0.36×0.27×0.21	0.41×0.30×0.25	0.40×0.30×0.08	0.30×0.24×0.12	0.33×0.27×0.13
crystal system	monoclinic	monoclinic	orthorhombic	monoclinic	triclinic
space group	Cc	$P2_1/c$	Ccca	$P2_1/n$	$P\bar{1}$
Formula	$C_{50}H_{50}O_3Si_2V_2$	$C_{24}H_{22}OSiV$	$C_{51}H_{45}OSi_2V_2$	$C_{28}H_{34}Si_2V_2$	$C_{36}H_{32}O_2Si_2V$
formula weight	856.96	405.45	831.68	544.61	603.74
a /Å	18.3952(10)	10.0867(9)	20.0119(10)	7.8240(5)	8.8101(6)
b /Å	10.0390(6)	25.1082(16)	34.109(2)	14.1395(9)	10.3305(8)
c /Å	23.7742(13)	7.9094(8)	12.1983(6)	23.7599(16)	17.7825(13)
β /°	108.341(4)	105.880(7)	90	94.410(8)	86.792(6)
volume /Å^3	4167.3(4)	1926.7(3)	8326.5(8)	2620.7	1492.01(19)
Z	4	4	8	4	2
density /mg/m^3	1.366	1.398	1.338	1.380	1.344
absorbtion coefficient	0.549 mm^{-1}	0.588 mm^{-1}	0.545 mm^{-1}	0.824 mm^{-1}	0.4400 mm^{-1}
F(000)	1792	844	3496	1136	630
Θ_{range}	1.80 to 26.25°	1.62 to 25.38°	2.04 to 25.00°	1.68 to 25.00°	2.14 to 26.28°
hkl index ranges	$-22\leq h\leq 22$, $-12\leq k\leq 12$, $-29\leq l\leq 29$	$-12\leq h\leq 11$, $-30\leq k\leq 30$, $-9\leq l\leq 9$	$-23\leq h\leq 23$, $-40\leq k\leq 40$, $-14\leq l\leq 14$	$-9\leq h\leq 9$, $-15\leq k\leq 16$, $-28\leq l\leq 20$	$-10\leq h\leq 10$, $-12\leq k\leq 12$, $-22\leq l\leq 22$
reflections collected	29818	16288	29322	11600	24390
indepentent reflections	8339 [R(int) = 0.0372]	3380 [R(int) = 0.0251]	3682 [R(int) = 0.0549]	4565 [R(int) = 0.0345]	5972 [R(int) = 0.0725]
obsd reflns [$I>2\sigma(I)$]	7944	3069	2680	3057	4311
reflections used	8399	3380	3682	4565	5972
largest diff. Peak/ hole /e.Å^{-3}	0.199 and −0.196	0.296 and −0.279	0.934 and −0.318	0.310 and −0.205	0.437 and -0.413
Parameters	715	332	353	368	375
GOF F^2	1.034	1.040	0.979	0.895	0.935
R1	0.0229	0.0274	0.0400	0.0326	0.0400
wR2	0.0595	0.0734	0.1021	0.0748	0.1099

Di([5]trovacenyl)tetraphenyl-disiloxane (3··) and ([5]trovacenyl)diphenylsiloxy-diphenylsilanol (5·)

To a solution of trovacene (**1**·) (983 mg, 4 mmol) in Et_2O (150 ml), n-butyl lithium (3.0 ml, 1.6 M/hexane, 4.8 mmol) was added and the mixture was stirred at room temperature overnight. Then 1,3-dichlorotetraphenyldisiloxane (0.45 ml, 1.19 mmol) in 20 ml Et_2O was added in 2 h with refluxing. After addition, the mixture was refluxed overnight with vigorous stirring. The suspension was filtered through Celite, the filtrate was evaporated under reduced pressure. Isolation by chromatography (Al_2O_3, 2.5×30 cm) gave **3**·· from a blue band eluted with toluene/Et_2O (3:1), followed by a pale blue band (EtOH: Et_2O = 1:1) which contains **5**·. The single crystals suitable for X-ray diffraction were grown from benzene/PE at 8 °C. **3**··: Yield: 314 mg (0.40 mmol, 20 %).

Elemental analysis: $C_{48}H_{42}OSi_2V_2$ (792.651): calcd C 72.73, H 5.30; found C 71.79, H 5.27 %. EI-MS (70 eV) *m*/*z* = 792 [M^+] (90 %), 701 [M^+-C_7H_7] (27 %), 142 [$C_5H_4VSi^+$] (25 %), 28 [$C_2H_4^+$] (100 %).

5·: Yield : 130 mg (0.22 mmol, 16 %).

Elemental analysis: $C_{36}H_{32}O_2Si_2V$ (603.506): calcd C 71.64, H 5.30; found C 70.43, H 5.22 %. EI-MS (70 eV) *m*/*z* = 603 [M^+] (100 %), 207 [TVC^+] (20 %).

Di([5]trovacenyl)tetramethyl-disiloxane (4··)

To a red-brown solution of lithiotrovacene (from trovacene (**1**·) 760 mg, 3.67 mmol and n-butyl lithium 2.3 ml, 3.68 mmol, 1.6 M/hexane) in Et_2O (150 ml), $ClMe_2SiOSiMe_2Cl$ (0.18 ml, 0.92 mmol) was added dropwise in 2 h and the mixture was refluxed for 3 h. The suspension was filtered through Celite and freed of all the volatiles. Purification was achieved by chromatography (Al_2O_3, 2×30 cm, toluene/PE and THF as eluents) to afford **4**·· as violet-blue solid. Yield: 290 mg (0.53 mmol, 29 %).

Elemental analysis: $C_{28}H_{34}OSi_2V_2$ (544.335): calcd C 61.78, H 6.25; found C 62.56, H 6.39 %. EI-MS (70 eV) *m*/*z* = 544 [M^+] (36 %); 452 [M^+-C_7H_7] (26 %); 91 [$C_7H_7^+$] (100 %).

Di([5]trovacenyldimethylsilyl)methane (6··)

$(ClSiMe_2)_2CH_2$ (0.16 ml, 0.8 mmol) was added dropwise to a solution of lithiotrovacene (from trovacene (**1**·) 670 mg, 3.24 mmol, n-butyl lithium 2 ml, 3.2 mmol, 1.6 M/hexane) at room temperature with vigorous stirring. After stirring overnight, the suspension was filtered through Celite, and the filtrate was evaporated in vacuum, the residue was purified by chromatography (Al_2O_3) to give **6**·· as pale blue solid. Yield: 140 mg (0.26 mmol 16 %).

Elemental analysis: $C_{29}H_{36}Si_2V_2$ (542.346): calcd C, 64.22; H, 6.69; found: C, 63.58; H, 7.26 %. EI-MS (70 eV) *m*/*z* = 542 [M^+] (100 %); 451 [M^+-C_7H_7] (50 %); 264 [TVC-$SiMe_2^+$] (4 %); 142 [$C_5H_4VSi^+$] (87 %); 116 [$C_5H_4V^+$] (18 %).

Acknowledgement. This work was supported by the Deutsche Forschungsgemeinschaft and the Fonds der Chemischen Industrie.

References and Notes

[1] Part 15: Ch. Elschenbroich, F. Lu, O. Burghaus, C. Pietzonka, K. Harms, *Chem. Comm*. **2007**, 3201.

[2] (a) V. Chandrasekhar, *Inorganic and Organometallic Polymers*, Springer, Berlin 2005; (b) P. Nguyen, P. Gómez-Elipe, I. Manners, *Chem. Rev.* **1999**, *99*, 1515; (c) R. J. Puddephatt, *Chem. Commun.* **1998**, 1055; (d) I. Manners, *Science* **2001**, *294*, 1664; (e) I. Manners, *Synthetic Metal Containing Polymers*, Wiley-VCH, Weinheim (2003); (f) G. R. Newkome, E. He, C. N.

Moorefield, *Chem. Rev.* **1999**, *99*, 1689; R. D. Archer, *Inorganic and Organometallic Polymers*, Wiley-VCH, Weinheim (2001); (g) M. S. Khan, M. R. A. Al-Mandhary, M. K. Al-Suti, A. K. Hisahm, P. R. Raithby, B. Ahrens, M. F. Mahon, L. Male, E. A. Marseglia, E. Tedesco, R. H. Friend, A. Köhler, N. Feeder, S. J. Teat, J. *Chem. Soc. Dalton Trans.* **2002**, 1358; (h) T. Yamamoto, K.-I. Sanechika, A. Yamamoto, M. Katada, I. Motoyama, H. Sano, *Inorg. Chim. Acta* **1983**, *73*, 75; (i) W. J. Patterson, S. P. McManus, C. U. Pittman, Jr., *J. Polym. Sci. Polym. Chem.* **1974**, *12*, 837; (j) T. Itoh, H. Saito, S. Iwatsuki, *J. Polym. Sci. Polym. Chem.* **1995**, *33*, 1589; (k) I. Manners, *Comprehensive Organometallic Chemistry. III* (R. M.: Crabtree, D. M. P. Mingos, Eds) 2007, *12*, 295.

[3] The number in brackets indicates the site of peripheral substitution: [5]trovacenyl derivatives are functionalized at the cyclopentadienyl ligand and [7]trovacenyl derivatives at the cycloheptatrienyl ligand.

[4] See ref. 1 and previous papers in the series Trovacene Chemistry.

[5] (a) H. Puff, K. Braun, H. Reuter, *J. Organomet. Chem.* **1991**, *409*, 119; (b) S. A. Bourne, L. R. Nassimbeni, K. Skobridis, E. Weber, *J. Chem. Soc. Chem. Commun.* **1991**, 282; (c) E. A. Babaian, M. Huff, F. A. Tibbals, D. C. Hrncir, *J. Chem. Soc. Chem. Commun.* **1990**, 306.

[6] P. D. Lickiss, *Adv. Inorg. Chem.* **1995**, *42*, 147.

[7] (a) G. A. Jeffrey, *An Introduction to Hydrogen Bonding*, Oxford University Press, New York P. 12, 1997; (b) J. E. Huheey, *Inorganic Chemistry*, 3rd Ed, Harper, Cambridge 1983.

[8] (a) D. Braga, F. Grepioni, E. Tedesco, *Organometallics* **1998**, *17*, 2669; (b) S. Harder, *Chem. Eur. J.* **1999**, *5*, 1852.

[9] K. L. Malisza, L. C. F. Chao, J. F. Britten, B. G. Sayer, G. Jaouen, S. Top, A. Decken, M. J. McGlinchey, *Organometallics* **1993**, *12*, 2462.

[10] C. Glidewell, D. C. Liles, *J. Chem. Soc. Chem. Commun.* **1977**, 632.

[11] F. Cervantes-Lee, H. K. Sharma, K. H. Pannell, A. Derecskei-Kovacs, D. S. Marynick, *Organometallics* **1998**, *17*, 3701.

[12] (a) C. Elschenbroich, M. Wolf, O. Schiemann, K. Harms, O. Burghaus, J. Pebler, *Organometallics* **2002**, *21*, 5810; (b) O. Kahn, *Molecular Magnetism*, VCH, Weinheim, 1993, Chapter 7.

[13] F. E. Mabbs, *Chem. Soc. Rev.* **1993**, *22*, 313.

[14] C. Elschenbroich, J. Plackmeyer, M. Nowotny, A. Behrendt, K. Harms, J. Pebler, O. Burghaus, *Chem. Eur. J.* **2005**, *11*, 7427.

[15] (a) W. Skibar, H. Kopacka, K. Wurst, C. Salzmann, K.-H. Ongania, F. F. de Biani, P. Zanello, B. Bildstein, *Organometallics* **2004**, *23*, 1024; (b) B. Bildstein, O. Loza, Y. Chizhov, *Organometallics* **2004**, *23*, 1825; (c) B. Bildstein, *Coord. Chem. Rev.* **2000**, *206-207*, 369. Note: [n-1] Cumulenes are defined as chains of n carbon atoms connected by (n-1) double bonds.

[16] C. Elschenbroich, J. Plackmeyer, M. Nowotny, K. Harms, J. Pebler, O. Burghaus, *Inorg. Chem.* **2005**, *44*, 955.

[17] S. Shambayati, S. L. Schreiber, J. F. Blake, S. G. Wierschke, W. L. Jorgensen, *J. Am. Chem. Soc.* **1990**, *112*, 697.

[18] J. R. Durig, M. J. Flanagan, V. F. Kalasinsky, *J. Chem. Phys.* **1977**, *66*, 2775.

[19] (a) R. B. King, F. G. A. Stone, *J. Am. Chem. Soc*. **1959**, *81*, 5263; (b) C. Floriani, *J. Chem. Soc. Dalton Trans.* **1976**, 1046.

[20] (a) U. Herzog, G. Rheinwald, *J. Organomet. Chem.* **2001**, *628*, 133; (b) G. Délris, M. Birot, J. Dunogués, B. Barbe, M. Pettaud, M. Lefort, *J. Organomet. Chem.* **1984**, *266*, 1.